Optimization of the terminations of an HTS cable operating on a DC railway network

Ghazi Hajiri, Kévin Berger, Jean Lévêque

Optimization of the terminations of an HTS cable operating on a DC railway network

Ghazi Hajiri, Kévin Berger, and Jean Lévêque

***Abstract*—In recent years, many projects have initiated to use superconducting cables to meet industrial challenges. More specifically, the integration of superconducting cables into DC railway network. This paper presents a comprehensive analysis of a single-pole superconducting cable and the losses caused by its associated components. The model used features a two-layer unipolar cable with a copper screen layer, a nominal current of 3 kA, and a nominal voltage of 1.5 kV. Furthermore, a coupled electric and thermal study is presented to assess the losses resulting from the terminations. The current flowing through the superconducting cable and terminations is simulated using a dynamic model of the railway network. Additionally, a detailed evaluation of the losses was conducted, along with a novel termination optimization approach which accounts for the true simulated current flow in the cable. This approach has considerably reduced the system's overall consumption, by 37%.**

***Index Terms*—Superconducting cable, terminations, electromagnetic modeling, thermal modeling, railway electrification, energy efficiency.**

I. Introduction

THE DC railway network operating at voltages below 1.5 kV is an important part of rail electrification, covering a substantial distance of 5,904 km, which represents about one quarter of the French national rail electrification [1]. Substations are installed at varying distances from 5 to 15 km, and the overhead conductors can have a cross-section of up to 1000 mm^2 [2]. However, this low-voltage supply configuration has a major drawback: voltage drops occur along the lines, which requires the installation of substations very close to each other. The NF EN 50163 standard requires the railway network to maintain a voltage of over 1000 V on the traction line at all times. In addition, the network is facing multiple challenges, including the increase in rail traffic. Between 1998 and 2008, rail traffic increased by 60% and is expected to quadruple by 2030. However, the length of rail lines has only marginally increased by 1.16% since 1997 [3]. Moreover, it is becoming increasingly difficult to install substations in densely populated areas.

To solve these problems and improve the quality of the power supply by reducing energy losses along the line in a limited space, the installation of superconducting power cables is an interesting solution. This approach uses second-generation (2G) High-Temperature Superconductor (HTS) tapes, capable of efficiently carrying large currents with practically zero electrical losses on DC networks where the di/dt variation of the current is very small. This is particularly relevant in the railway context, where the current is generally continuous, but where variations can occur when trains accelerate or brake. Currently, commercially available 2G superconducting tapes exhibit an engineering current density of 300 A/mm^2 when operating in the self-field at liquid nitrogen temperatures (77 K). This represents a current carrying capacity around 300 times greater than that of a copper conductor, according to DIN43671. In addition, this technology offers a compact and flexible system that can effectively meet the demands of the urban environment.

These significant advantages have prompted Société Nationale des Chemins de Fer Français (SNCF) to explore a new solution based on the use of superconducting cables to meet the increasing energy constraints and demands of rail traffic. In 2022, the “SuperRail” project was launched to integrate two 80-meter long superconducting cables at the Montparnasse train station in Paris. This project will mark the first commercial use of superconducting cables on the French rail network and has received government support as part of the France 2030 program [4].

In this context, this paper focuses on the evaluation of losses in a superconducting system for the railway application. Furthermore, a fine optimization of the superconducting system requires the simulation of indispensable parameters such as the superconducting cable, its terminations and the DC railway network. This paper is based on a thorough modeling of the entire electrical system, with the aim of reducing the energy consumption of the cooling system and optimizing its energy efficiency. The paper is divided into several sections, with an introduction and conclusion, and three main sections. Section II deals with the design of a superconducting facility, while section III deals with Multiphysics modeling. The latter includes a Finite Element Model of the cable (FEMc), a Finite Element Model of the cable termination (FEMt), and an Electrical Model of the railway network (EMrn), which simulates substations, trains, and their movement. Section IV of this paper presents a realistic case study involving several trains. In this context, we examine the losses generated by each component of the superconducting

This research was supported by the SuperRail project funded by BPI France through the PIA4 and France 2030 programs.

Ghazi Hajiri, Kévin Berger and Jean Lévêque are with the University of Lorraine, GREEN, F-54000 Nancy, France (e-mail: surname.name@univ-lorraine.fr).

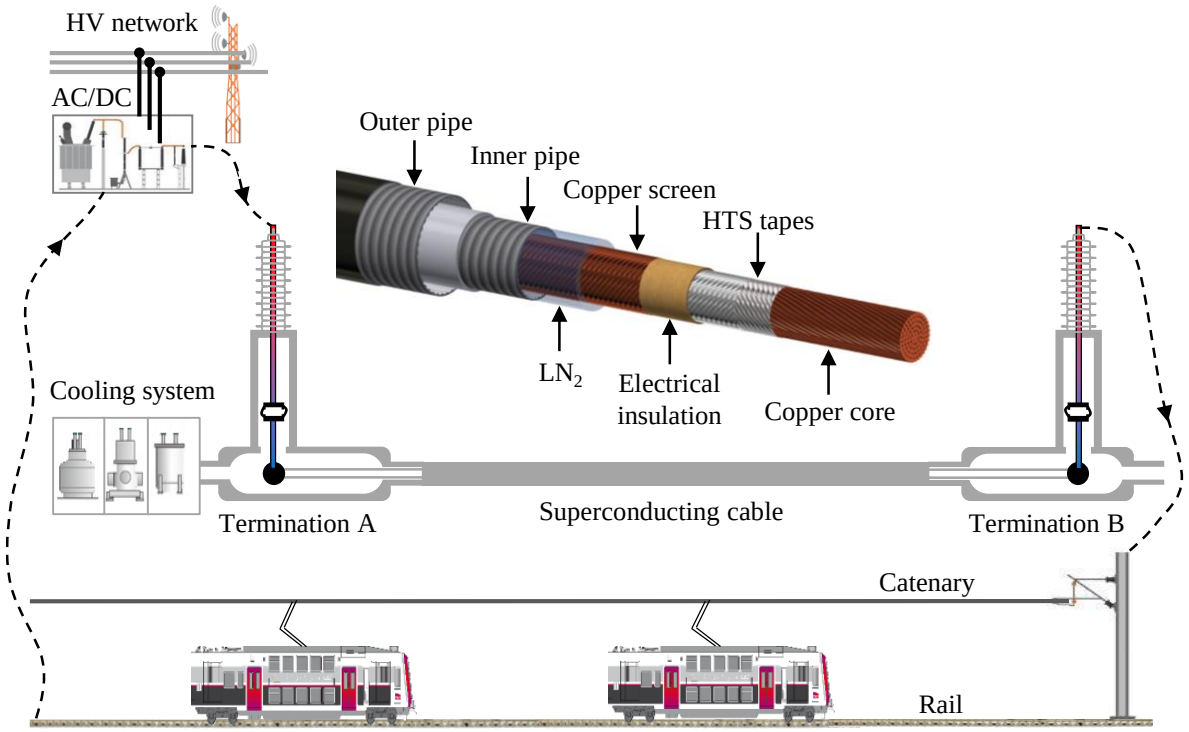

Fig. 1. Diagram representing the introduction of a superconducting cable in the railway network and a complete 3D view of a superconducting coaxial cable with its different layers. The return of the traction current is done through the rails.

system. In addition, we introduce a new approach to optimize the terminations of the superconducting cable specifically dedicated to the DC railway network.

II. Description of a Superconducting Cable System

A superconducting system for power grid applications consists of several components, the main one being the superconducting cable, as shown in Fig. 1. An HTS cable consists of several concentric layers of tapes wound on a twisted copper core also called “stabilizer”. The sizing of the cable was performed using the algorithm outlined in [5]. The pole of the cable is placed above the stabilizer. In the example considered, the cable is 100 m long and consists of 24 superconducting tapes arranged in two layers for a total critical current I_c of the cable of 4.4 kA, defined for an electric field of 1 µV/cm. This pole is usually covered with a few millimeters of Polypropylene laminated paper immersed in liquid nitrogen, used for its good insulating properties and its behavior in liquid nitrogen. For a 1.5 kV DC railway network, a paper thickness of 1 to 2 mm is sufficient to maintain a minimum insulation distance under all conditions of use. The top layer, also called “screen”, consists of several copper tapes grounded at the ends of the cable. This set of layers is then inserted into a flexible cryostat which allows the circulation of liquid nitrogen. The cooling of the cables can be done either inside the cable itself (LN_2 inlet and outlet are in the same cable), or by adding an external pipe to ensure the return of the liquid nitrogen [6]. The second element of a superconducting system is the cooling system including the circulation pumps for the liquid nitrogen. Its main role is to maintain the temperature of the superconducting cable in the range of 68 to 78 K, as well as a pressure range of 3 to 15 bar [7]. In an HTS cable operating in direct current, the main losses come from the cable cryostat and are of the order of 1.2 W/m. Finally, a superconducting system also requires terminations which are located at each end of the cable and ensure the connection of the cable to the electrical network. They also allow the connection between the different liquid nitrogen pipes, and make the link between the hot and cold elements of the system. Terminations are complex technical assemblies. They are generally the well-guarded know-how of superconductor cable companies.

III. Modelling of a Superconducting Cable System

A. Finite Element Model of the cable (FEMc)

The FEMc aims to calculate the electrical losses of the cable using an electromagnetic calculation method based on the **T-A** formulation of Maxwell's equations [8]. This is the most efficient formulation for superconducting tapes and offers both good computation time and good accuracy of results compared to the existing **H** formulation [9]. The current vector potential **T** is solved exclusively in the Ω_{HTS} superconducting domain (superconducting layer of each individual tape), while the magnetic vector potential **A** is solved in the complementary domain called the air domain or Ω_A. The air domain consists of clusters or any other material that is not the superconducting material. The current density **J** of the superconductor is deduced from $\mathbf{J} = \nabla \times \mathbf{T}$. The electric field **E** is determined by the magnetic induction **B** according to Faraday's law. In addition, a study of the

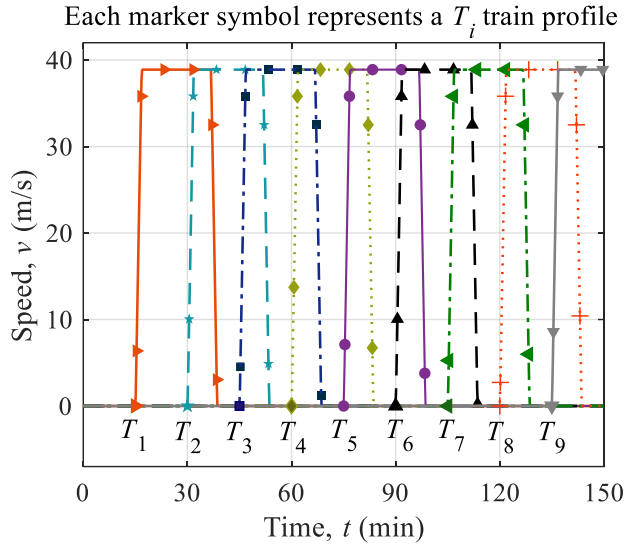

Fig. 2. Dynamic profile (speed) of the trains as a function of time, the instants T_1, T_2, T_3, T_4, T_5, T_6, T_7, T_8, T_9 represent the departure of the trains.

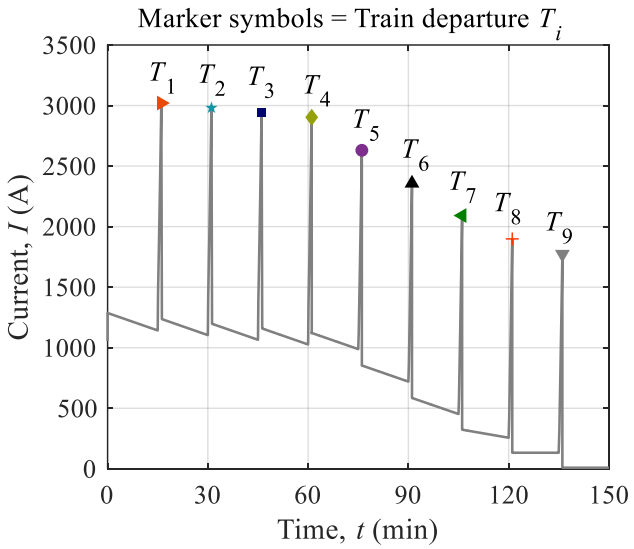

Fig. 3 Current flowing in the superconducting cable as a function of time, instants T_1, T_2, T_3, T_4, T_5, T_6, T_7, T_8, T_9 represent the departure of the trains.

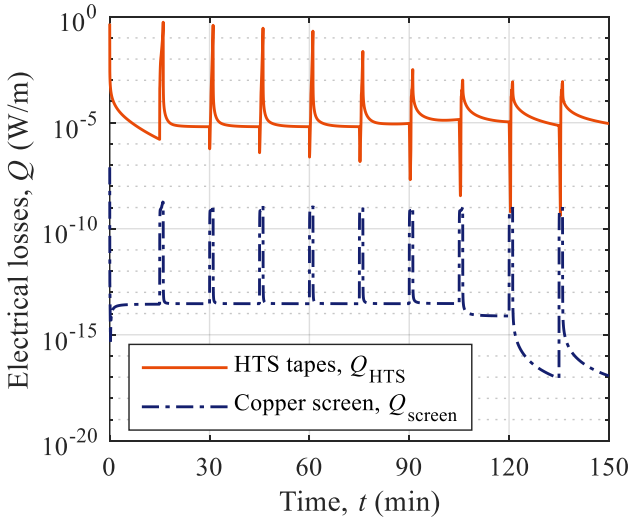

Fig. 4. Electrical losses of the superconducting cable and the copper screen versus time.

induced currents and electrical losses of the copper screen layer is taken into account. The FEMc model also takes into account nonlinear electrical parameters related to superconductivity, such as the power law $E(J)$ [10] and the dependence of the critical current density $J_c(B, \theta)$ on the magnetic field and its application angle [11]. More details on the implementation of the FEMc are described in section 3.4 of [7].

B. *Finite Element Model of the cable termination (FEMt)*

As mentioned previously, the terminations are the source of multiple losses: mainly by thermal conduction and Joule effect. The FEMt here is a 1D unidirectional thermoelectric model. In fact, in the case of DC, the distribution of the current is uniform over the entire conductor section, which makes this approach appropriate. The cooling of the termination is considered through a convective flux depending on the temperature $q_0(\theta)$, the choice of this cooling flux will be discussed in subsection IV.B. The thermal and electrical properties of the materials used in this document such as copper, aluminum and brass are given in [12] and obviously depend on temperature.

C. *Electrical Model of the railway network (EMrn)*

The objective of the EMrn is to simulate the railway network in dynamic regime. To do so, the three main components of the railway electrical system are: substations, trains and the evolution of the line impedance with train traffic. The substation model contains a transformer whose primary windings are supplied with a line voltage of 20 kV, generating 4.5 MW of power under load. In addition, a double diode Graetz bridge is present, with a nominal voltage of 1.5 kV and a continuous current rating of 3 kA. An inductance at the output of the substation is introduced to smooth the current variation (di/dt) due to transients induced by the acceleration and deceleration of the train. The calculation of the electrical power of the trains is obtained from the calculation of the sum of the traction forces necessary to ensure its movement and the electrical power of the auxiliaries (lighting, air conditioning, etc.). The management of the line impedance is calculated at each time step according to the position of the train during its mission in order to take into account the movement of the trains with respect to the electrical network [7].

IV. Case Study and Discussion

The case study scenario involves the departure of nine trains from the HTS cable connection point, see Fig. 2. This is a typical scenario representing the departures of trains stored on a track over the course of a morning. The train departures are spaced 15 minutes apart. Each train leaves the substation accelerating at 70 km/h/min for 2 minutes, then maintains a constant speed of 140 km/h for 20 minutes. After 65 seconds, the train leaves the 700-meter section powered by the HTS cable and its power consumption is then taken from another substation. The train then decelerates to 70 km/h/min for 2 minutes. Before the

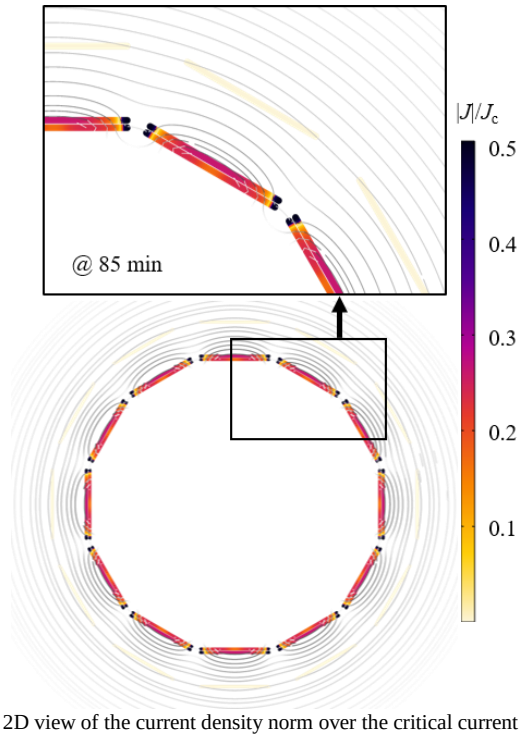

Fig. 5. 2D view of the current density norm over the critical current density $|J|/J_c$, as well as the magnetic field lines in the cable at t = 85 min.

departure of the train, a parking process is considered, consisting of three distinct phases. The first phase, called Pre-Conditioning (PC), involves a power supply of 450 kW for the train for a period of 30 minutes. The second phase is the transition period between the Pre-Conditioning regime and the Service Maintenance (SM) regime, during which the train power decreases linearly for 60 minutes until it reaches 210 kW, which is the power required to ensure the SM regime. In the simulation, at $t = 0$, only five trains are powered. Train T_1 is considered to be in the MS regime, while train T_2 is in the transition phase between the PC and MS regime, consuming 330 kW of power. On the other hand, trains T_3, T_4 and T_5 are in PC regime. After the departure of each train T_1, T_2, T_3, T_4, a new train is fed from the substation, respectively T_6, T_7, T_8 and T_9. Fig. 3 illustrates the temporal evolution of the current in the superconducting cable. At each acceleration of the trains, a current peak appears, reaching up to 3 kA when the first train starts.

A. *Losses of the HTS cable*

The electrical losses in the superconducting tapes and the resistive screen are shown in Fig. 4. The total of these losses is less than 0.5 W on average during the operating cycle, which remains negligible compared to the cryostat losses, estimated at 120 W for a 100 m cable. Fig. 5 shows an example of distributions of the norm of the current density $|J|$ divided by the critical current density J_c in the superconducting layers calculated by FEMc at t = 85 min. We observe that the current is distributed non-uniformly in the superconducting layers. This distribution results from the nonlinear behavior of the superconductor resistivity. Indeed, when the transport current is lower than the critical current I_c of the cable, the current starts to penetrate the superconducting layers at both ends until it reaches the center of the tapes for values close to I_c. Fig. 5 also shows that the

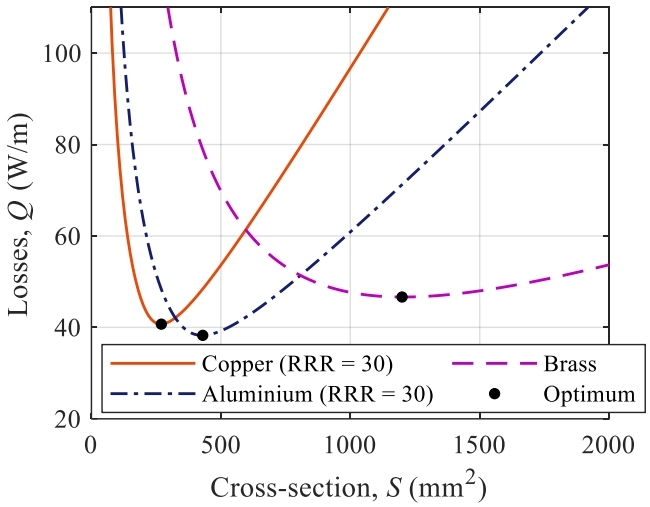

Fig. 6. Losses of a termination per meter as a function of the conductor section, for a transport current equal to 1 kA and in adiabatic regime.

magnetic field lines have a substantial component perpendicular to the tapes, due to the non-negligible space between them.

It can easily be established that for a superconducting cable operating on a DC network, the losses of the cable cryostat are predominant. Examples include the addition of super-insulating layers or improving the quality of the vacuum separating the inner and outer walls of the cable cryostat. Further reducing these losses is very difficult and would require the development of solutions that are not yet industrialized. Therefore, the only remaining losses to be optimized to reduce losses in the HTS cable system are those of the terminations.

B. *Termination losses*

As already mentioned, the termination of a superconducting cable is the place where various losses occur. There are Joule losses associated with the resistive conductor, as well as conduction losses. Indeed, the termination is constantly connected to two different temperatures at each end. One is at the ambient temperature of the power system (assumed to be 300 K), while the other is at the cryogenic temperature of 68 K in our case. Therefore, a heat flux is transferred towards the cable. Losses from the termination cryostat are also an additional source of losses. In this 1.5 kV low-voltage application, the terminations are relatively small compared with those required for high-voltage cables. These losses are estimated to be about 20 W per termination and cannot be easily reduced. Therefore, we are mainly interested in reducing the Joule and thermal conduction losses. The parameters for reducing termination losses are therefore the conductor cross-section, the nature of the material and its length. Fig. 6 shows the losses of a termination as a function of the conductor cross-section for a nominal current of 1 kA and for three different materials: copper, aluminum and brass. In this example, there is no heat exchange between the conductor and its external environment, i.e. adiabatic regime. Fig. 6 shows that a compromise is necessary in order to optimize the conductor cross-section. Indeed, decreasing the conductor cross-section causes an increase in the termination losses due to Joule effect losses, while increasing the conductor cross-

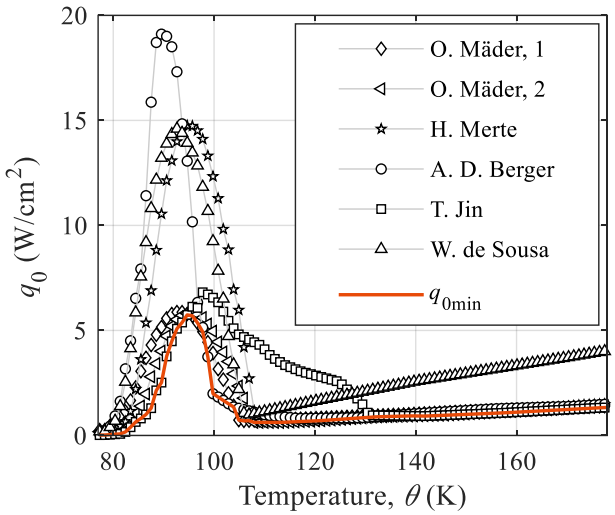

Fig. 7. Review of measured heat fluxes between a solid and liquid nitrogen at 77.3 K: O. Mäder, 1 [13], O. Mäder, 2 [13], H.Merte [14], A.D. Berger [15], T. Jin [16], W. de Soussa [17].

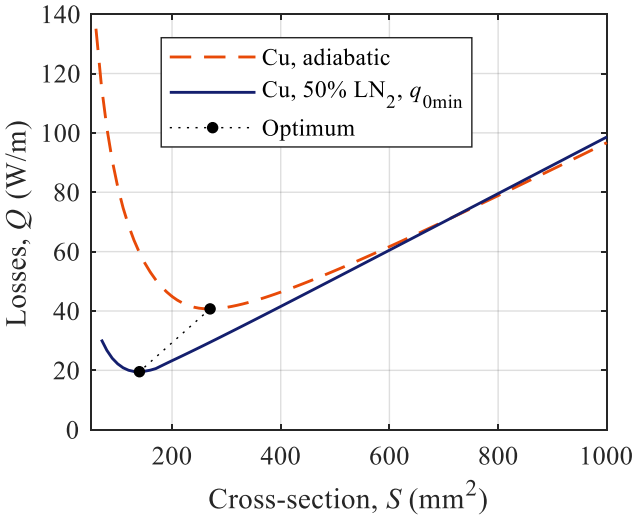

Fig. 8. Losses of a termination per meter as a function of the conductor section, for a transport current equal to 1 kA for an adiabatic regime and a 50% cooling of the copper conductor.

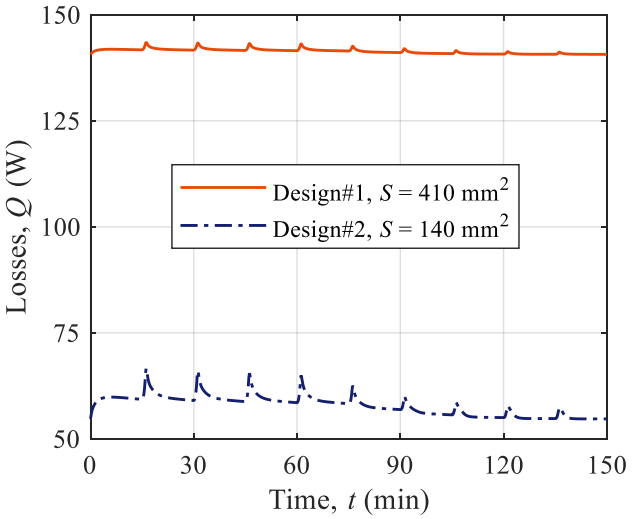

Fig. 9. Losses of a termination as a function of time for the operating cycle shown in Fig. 3.

section also increases the termination losses due to thermal conduction losses. Thus, there is a trade-off to be found to minimize the losses. The optimum point for the three materials is reached at 40.7 W/m, 38.2 W/m and 46.6 W/m for cross-sections of 270 mm^2 in copper, 430 mm^2 in aluminum and 1200 mm^2 in brass respectively, for a conductor length of 1 m. Overall, the use of aluminum slightly reduces the optimum point compared to copper, with a difference of 2.5 W/m. However, a larger cross-sectional area is required for aluminum, which will tend to magnify the size of the cryostat and thus increase its radiation losses. Therefore, we chose to keep copper as the material in this study.

To simulate a more realistic and effective scenario, part of the termination conductor is immersed in liquid nitrogen. The level of immersion in liquid nitrogen can vary depending on the design of the termination [13]. In this study, we consider that half of the termination conductor is in liquid nitrogen. In addition, in order to take account of this cooling, various heat flux measurements currently available in the literature between a solid and liquid nitrogen have been brought together and shown in Fig. 7 [14]–[18]. It is complex to compare these results as they depend on several parameters such as the shape and geometry of the samples, the immersion level of the sample, as well as its orientation in the liquid nitrogen bath, e.g. vertical or horizontal. In the process of sizing the terminations, using Fig. 7 a minimum convective heat flux q_{0min} (in orange) was defined in order to obtain an overestimate of the termination losses. As shown in Fig. 8, taking this cooling into account, the minimum losses of a termination have been reduced by two, as well as the conductor cross-section. These losses are now equal to 20 W/m for a copper cross section of 140 mm^2. An auxiliary system must be added to cool each termination by liquid nitrogen convection. This basically consists of a tank and a gas exhaust. Depending on site accessibility and maintenance constraints, more complex cooling systems may be considered, such as adding a sub-cooler or other active cooling system like a cryocooler.

Based on the same principle of termination optimization, two termination design methods are now discussed:

- The first one, called "Design#1", is based on the optimization of the termination for an operating current equal to the substation rated current, i.e., 3 kA, i.e., an optimal conductor section of 410 mm^2 and 40 cm of length.
- The second one, Design#2, is based on the optimization of the termination for an operating current equal to the average current I_{avg} predicted by the model presented in section III and illustrated in Fig. 3. I_{avg} is equal to 1 kA, implying an optimal conductor section of 140 mm^2 and 40 cm of length.

Fig. 9 shows the evolution of the losses of a single termination over time for both Design#1 and #2 and for the cycle shown in Fig. 3. It can be seen that the average electrical and thermal losses of a single termination amount to 142 W for Design#1 and 58 W for Design#2. This is because using the average current value rather than the nominal value allows the conductor cross-section to be reduced and, therefore, the conduction losses to be reduced. A 59.2% reduction in termination losses

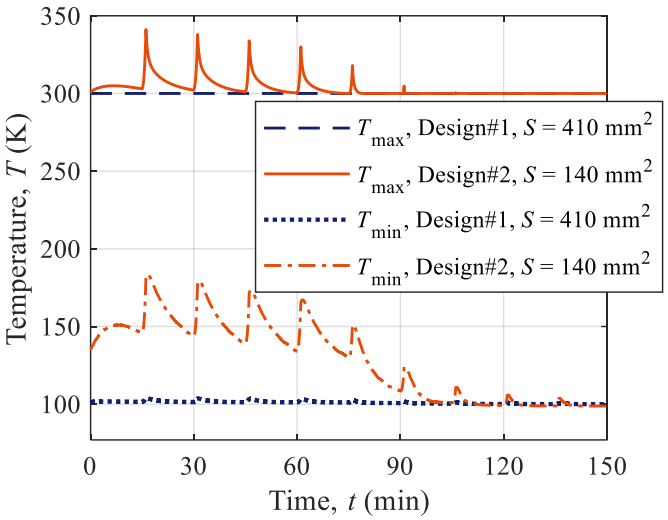

Fig. 10. Maximum (T_{max}) and minimum temperatures (T_{min}) over time for both designs. These temperatures are calculated for the part of the terminations that is not immersed in liquid nitrogen.

can thus be achieved. At this stage, it therefore seems very important to get the message across, both to the termination provider and to the user, that these must be optimized for the effective current and not for the maximum current of the cable.

C. *Thermal analysis of terminations*

Fig. 10 illustrates the variation over time of the maximum temperature (T_{max}) and minimum temperature (T_{min}) at the terminations for both designs. T_{min} represents the minimal temperature of the part of the conductor that is not immersed in liquid nitrogen. In Design#1, both temperatures T_{max} and T_{min} remain almost constant at 300 K and 100 K. An increase of only 5 K was observed on T_{min}. Indeed, during the optimization of the termination with the FEMt, a section of 410 mm^2 was obtained to ensure a gradually decreasing thermal gradient from 300 K to 77 K for a transport current of 3 kA.

On the other hand, in Design#2, temperature rises occur during the inrush of current. These temperature peaks are linked to the fact that the conductor is designed for a current of 1 kA. When the transport current exceeds this value, temperature rises occur. However, these are far from being critical or destructive to the conductor. In Design#2, T_{max} is in the range of 300 K to 340 K while T_{min} is in the range of 98 K to 180 K. This causes no particular problems for the operation of the termination or the superconducting cable system in general.

D. *Choice of cold source and energy consumption*

The system's overall energy consumption is highly dependent on the choice of cold source for the cable, i.e. the type of cooling system used. In addition, the choice of cold source is based on criteria such as operating temperature, size, power, maintenance costs and service life. As part of the cooling of superconducting cables with liquid nitrogen, the energy consumption of different cooling systems was compared, namely:

- Stirling Cryocooler is an old and well-known technology. It provides 1 W of cooling power while consuming around 18.3 W of electricity [19]. The maintenance-free lifespan of a Stirling machine is approximately 60,000 hours [20].
- Pulse Tube Cryocooler technology is a variation of the Stirling cycle, where the displacer is a passively phased gas mass. A single-stage Pulse Tube Cryocooler can deliver 1 W at a temperature of 70 K while consuming 12.5 W of electricity, with a Carnot efficiency of around 12.5% at the temperature of liquid nitrogen [21]. Similar to the Stirling Cryocooler, the drawback is the regular maintenance required for compressors and rotary joints.
- Turbo-Brayton is a high-speed machine that combines active elements such as the compressor, motor, and turbo-expander on the same shaft. This enables a more compact system with higher efficiencies [22], achieving a Carnot efficiency greater than 30%. The Turbo-Brayton typically consumes 11.6 W of electrical energy to produce 1 W of cold power [19], making it more economical than systems based on the Inverse Brayton Cycle and the Stirling Cryocooler. Models with cooling powers ranging from 10 kW to 77 kW are currently available on the market [23].

TABLE I
AVERAGE LOSSES OF THE ENTIRE SUPERCONDUCTING CABLE SYSTEM FOR BOTH DESIGNS AND ENERGY CONSUMPTION INCLUDING THE COOLING SYSTEM.

Component	Type of losses	Design#1	Design#2
Superconducting cable	Cable cryostat	120 W	
	Electrical	0.5 W	
1x termination	Termination cryostat	20 W	
	Electrical and thermal	142 W	58 W
Total		444.5 W	276.5 W
Energy consumption at room temperature	Stirling Cryocooler	20.3 kWh	12.6 kWh
	Single Stage Pulse Tube	22.2 kWh	13.8 kWh
	Turbo-Brayton	12.9 kWh	8 kWh

In this section, we seek to evaluate the overall energy consumption of the system including the cooling system, for both Design#1 and #2. Table 1 summarizes the average losses of the entire superconducting cable system for the case under study and the total energy consumption brought to room temperature, including the cooling system. For a superconducting system with terminations based on Design#1, the total losses are on average equal to 444.5 W, and the losses generated by the terminations account for 72.9% of the total system losses, as shown in Fig. 11. On the other hand, with the terminations based on Design#2, total system losses are reduced to 276.5 W. Furthermore, according to Fig. 12, losses from Design#2 terminations now account for only 56.4% of the total system losses. According to Table 1, Turbo Brayton remains the most effective system in terms of cooling, with a consumption of 8 kWh for the Design#2 case, while the Pulse Tube and Stirling consume 12.6 kWh and 13.8 kWh, respectively. It should be noted that the Pulse Tube is not a viable solution for cables longer than 1 km, as this technology can currently only provide limited cooling power, in the order of a few kilowatts. In this case, it is more suitable to use systems such as Stirling and Turbo-Brayton machines.

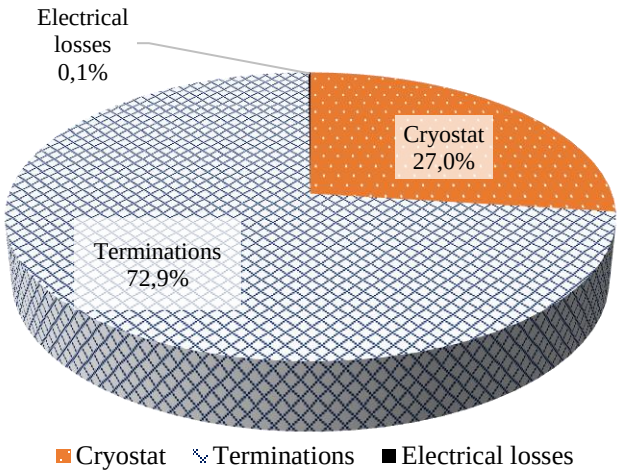

Fig. 11. Loss allocation of the superconducting cable and its terminations for Design#1.

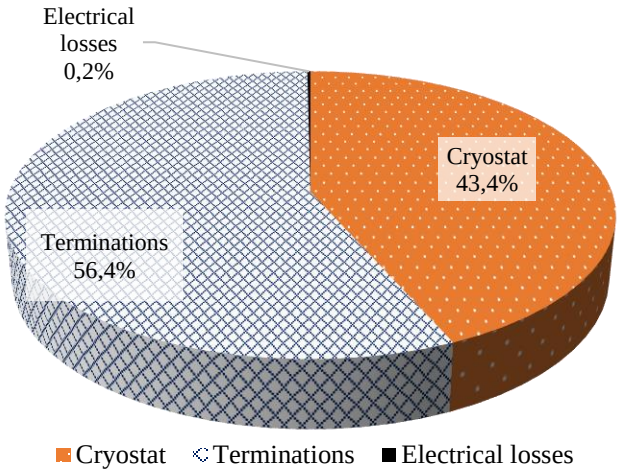

Fig. 12. Loss allocation of the superconducting cable and its terminations for Design#2.

V. Conclusion

In this study, we performed a loss assessment of a superconducting cable system for a real application case on a 1.5 kV DC railway network. Three models were developed, including two finite element models (FEMc and FEMt) for the cable and terminations respectively, as well as an electrical circuit type model EMrn to evaluate the dynamic behavior of the cable in the railway network.

In addition, a case study of a railway scenario was carried out to assess the losses of the superconducting system as a whole. In this part, a new termination optimization approach was proposed and compared to a classical optimization, with operation temperature between 68 K and 78 K. The results showed that this approach allowed to reduce the total losses of the system by about 37%. Furthermore, the overall energy consumption of the system at room temperature was examined by considering different cooling systems for the cable. The use of a Turbo-Brayton was studied, revealing a consumption of 12.9 kWh for Design#1 and 8 kWh for Design#2.

In conclusion, this study highlighted some important points. On the one hand, an optimized approach to termination based on the effective current during a daily scenario can lead to a significant reduction in total system losses. On the other hand, the judicious choice of the cooling system, such as the Turbo-Brayton, can contribute to further reduce the energy consumption of the system. These results open new perspectives for the optimization of superconducting systems in railway networks, by fostering better energy efficiency and loss reduction.

Acknowledgment

This work is funded by the France 2030 program through the Banque Publique d'Investissement (BPI). The authors would also like to express their gratitude to all the partners of the SuperRail project, namely SNCF Réseau, Nexans, Absolut System and CentraleSupélec, for their constructive discussions and the information they provided us on the French traction network and trains. Their contribution was essential to the success of this study.

References

[1] A. Steimel, “Under Europe’s incompatible catenary voltages a review of multi-system traction technology,” in *Railway and Ship Propulsion 2012 Electrical Systems for Aircraft*, Oct. 2012, pp. 1–8. doi: 10.1109/ESARS.2012.6387460.

[2] J. Fabre *et al.*, “Characterization and Implementation of Resonant Isolated DC/DC Converters for Future MVdc Railway Electrification Systems,” *IEEE Transactions on Transportation Electrification*, vol. 7, no. 2, pp. 854–869, Jun. 2021, doi: 10.1109/TTE.2020.3033659.

[3] J.-L. Legrand, “Écomobilité dans la transition énergétique,” *Techniques de l'Ingénieur [BE 6002]*, Mar. 2020, doi: 10.51257/a-v1-be6002.

[4] “Le Gouvernement annonce les 7 premiers lauréats de l’Appel à Manifestation d’Intérêt (AMI) du CORIFER,” Ministères Écologie Énergie Territoires, Mar. 2022. Accessed: May 14, 2023. [Online]. Available: https://www.ecologie.gouv.fr/gouvernement-annonce-7-premiers-laureats-lappel-manifestation-dinteret-ami-du-corifer

[5] G. Hajiri, K. Berger, R. Dorget, J. Lévêque, and H. Caron, “Thermal and Electromagnetic Design of DC HTS Cables for the Future French Railway Network,” *IEEE Transactions on Applied Superconductivity*, vol. 31, no. 5, Art. no. 5400208, Aug. 2021, doi: 10.1109/TASC.2021.3059598.

[6] G. Hajiri, K. Berger, R. Dorget, J. Lévêque, and H. Caron, “Design and modelling tools for DC HTS cables for the future railway network in France,” *Supercond. Sci. Technol.*, vol. 35, no. 2, Art. no. 024003, Jan. 2022, doi: 10.1088/1361-6668/ac43c7.

[7] G. Hajiri, K. Berger, F. Trillaud, J. Lévêque, and H. Caron, “Impact of Superconducting Cables on a DC Railway Network,” *Energies*, vol. 16, no. 2, Art. no. 776, Jan. 2023, doi: 10.3390/en16020776.

[8] Y. Wang, M. Zhang, F. Grilli, Z. Zhu, and W. Yuan, “Study of the magnetization loss of CORC® cables using a 3D T-A formulation,” *Supercond. Sci. Technol.*, vol. 32, no. 2, Art. no. 025003, Jan. 2019, doi: 10.1088/1361-6668/aaf011.

[9] F. Huber, W. Song, M. Zhang, and F. Grilli, “The T-A formulation: an efficient approach to model the macroscopic electromagnetic behaviour of HTS coated conductor applications,” *Supercond. Sci. Technol.*, vol. 35, no. 4, Art. no. 043003, Mar. 2022, doi: 10.1088/1361-6668/ac5163.

[10] J. Duron, F. Grilli, B. Dutoit, and S. Stavrev, “Modelling the E–J relation of high-Tc superconductors in an arbitrary current range,” *Physica C: Superconductivity*, vol. 401, no. 1–4, pp. 231–235, Jan. 2004, doi: 10.1016/j.physc.2003.09.044.

[11] S. C. Wimbush and N. M. Strickland, “A Public Database of High-Temperature Superconductor Critical Current Data,” *IEEE Transactions on Applied Superconductivity*, vol. 27, no. 4, pp. 1–5, Jun. 2017, doi: 10.1109/TASC.2016.2628700.

[12] B. Baudouy, G. Defresne, P. Duthil, and J.-P. Thermeau, “Propriétés des matériaux à basse température,” *Techniques de l'Ingénieur [BE 9811]*, Oct. 2014, doi: 10.51257/a-v1-be9811.

[13] L. Ren, Y. Tang, J. Shi, and F. Jiao, “Design of a Termination for the HTS Power Cable,” *IEEE Transactions on Applied Superconductivity*, vol. 22, no. 3, Art. no. 5800504, Jun. 2012, doi: 10.1109/TASC.2012.2191482.

[14] O. Mäder, “Simulationen und Experimente zum Stabilitätsverhalten von HTSL-Bandleitern,” Doctoral dissertation, Karlsruher Institut fur Technologie, May 2012. Accessed: May 14, 2023. [Online]. Available: https://publikationen.bibliothek.kit.edu/1000028713.

[15] H. Merte, “Incipient and steady boiling of liquid nitrogen and liquid hydrogen under reduced gravity,” Technical Report no. 7, The University of Michigan, Nov. 1970. Accessed: May 14, 2023. [Online]. Available: http://deepblue.lib.umich.edu/handle/2027.42/6581.

[16] A. D. Berger, “Stability of superconducting cables with twisted stacked YBCO coated conductors,” PSFC Report, Massachussets Institude of Technology, 2012. Accessed: May 14, 2023. [Online]. Available: https://dspace.mit.edu/handle/1721.1/93343.

[17] T. Jin, J. Hong, H. Zheng, K. Tang, and Z. Gan, “Measurement of boiling heat transfer coefficient in liquid nitrogen bath by inverse heat conduction method,” *J. Zhejiang Univ. Sci. A*, vol. 10, no. 5, Art. no. 5, May 2009, doi: 10.1631/jzus.A0820540.

[18] W. T. B. De Sousa, A. Polasek, R. Dias, C. F. T. Matt, and R. De Andrade, “Thermal–electrical analogy for simulations of superconducting fault current limiters,” *Cryogenics*, vol. 62, pp. 97–109, Jul. 2014, doi: 10.1016/j.cryogenics.2014.04.015.

[19] A. P. Malozemoff, J. Yuan, and C. M. Rey, “5 - High-temperature superconducting (HTS) AC cables for power grid applications,” in *Superconductors in the Power Grid*, C. Rey, Ed., Cambridge, U.K.: Woodhead Publishing, 2015, pp. 133–188. doi: 10.1016/B978-1-78242-029-3.00005-4.

[20] M. Hanes, “Performance and Reliability Improvements in a Low-Cost Stirling Cycle Cryocooler,” in *Cryocoolers 11*, R. G. Ross, Ed., Boston, MA: Springer US, 2002, pp. 87–95. doi: 10.1007/0-306-47112-4_11.

[21] A. Caughley *et al.*, “Commercialisation of Pulse Tube cryocoolers to produce 330 W and 1000 W at 77 K for liquefaction,” *IOP Conf. Ser.: Mater. Sci. Eng.*, vol. 101, no. 1, p. 012060, Nov. 2015, doi: 10.1088/1757-899X/101/1/012060.

[22] N. Nakamura, M. Shimoda, H. Yaguchi, and T. Mimura, “Turbo-Brayton Refrigerator of Yokohama HTS Cable Project,” presented at the 2nd International Workshop on Cooling Systems for HTS Applications (IWC-HTS), Karlsruhe, Germany, 13-15 Sept. 2017. Accessed: May 19, 2023. [Online]. Available: https://publikationen.bibliothek.kit.edu/1000075559

[23] S. Ozaki, H. Hirai, M. Hirokawa, and H. Kobayashi, “Development of 10 kW turbo-Brayton refrigerator for HTS power applications,” *IOP Conf. Ser.: Mater. Sci. Eng.*, vol. 502, no. 1, p. 012008, Apr. 2019, doi: 10.1088/1757-899X/502/1/012008.